

Calibration Strategies for Optical Underwater 3D-Scanners

Christian Bräuer-Burchardt¹, Roland Ramm¹, Matthias Heinze¹, Peter Kühmstedt¹, Gunther Notni^{1,2}

¹ Fraunhofer Institute for Applied Optics and Precision Engineering, 07745 Jena, Germany – christian.braeuer-burchardt@iof.fraunhofer.de, [roland.ramm, matthias.heinze, peter.kuehmstedt, gunther.notni]@iof.fraunhofer.de

² Machine Engineering Faculty, Technical University Ilmenau, Ehrenbergstraße 29, D-98693 Ilmenau, Germany; gunther.notni@tu-ilmenau.de

Keywords: Underwater 3D Scanning, Camera Modeling, Underwater Camera Calibration.

Abstract

The precise three-dimensional (3D) reconstruction of underwater objects is required in many different applications. Optical systems are gaining popularity due to their high accuracy potential. As a result, calibration of these systems for underwater use is becoming increasingly important. Several approaches for high quality calibration of optical 3D sensors based on stereo cameras are introduced and compared. Because of the transition of the vision rays between the media air, glass, and water, the calibration of optical underwater 3D scanners is challenging. The presented calibration strategies, including expanded advanced pinhole camera modeling, explicit ray refraction modeling, and systematic error compensation by correction functions are described and discussed. The presented strategies provide high accuracy and robustness on the one hand, and practicable usage and pleasant handling on the other hand. Requirements, advantages and limitations of the different strategies are discussed.

1. Introduction

Precise underwater 3D measurements become more and more important. According to the specific application, several image generating principles are used, such as laser scanning, photogrammetric systems, or sonar-based measurement systems. Each of the principles has its advantages and disadvantages. Optical 3D scanning supported by structured illumination enables the highest measurement accuracy, good completeness and high robustness of the measurements (Bräuer-Burchardt et al. 2022a). These requirements are essential for certain inspection tasks, such as for the evaluation and quantification of small cracks and scratches at sensitive surfaces of e.g. pipelines, energy generating structures, or ships' hulls. One essential component of a high precision 3D measurement system is the complete calibration process, which generates a set of calibration parameters according to an appropriate camera model.

Underwater calibrations for stereo systems are very demanding compared to air calibrations due to challenging conditions such as poor visibility and the refraction of the lines of sight on the different media. Additionally, common pinhole camera modeling is not completely valid. Hence, the calibration process is particularly important. Therefore, many studies have addressed this issue in the past. Various theories and approaches have been presented, each of which is adapted to the existing constraints and specific use cases, while also considering the requirements for robustness and accuracy. A detailed overview of existing calibration strategies for optical underwater 3D measurement systems are given by (Menna, 2018) or (Shortis, 2019).

The challenges lie in the construction of a robust calibration method and a manageable 3D calculation procedure. In this work, we will give a practicable approach for both problems. We present three approaches for the underwater calibration of stereo scanners, each of which aims to achieve a good compromise between accuracy and robustness on the one hand, and manageability and cost-effectiveness on the other. Advantages and limitations of the certain strategies are presented and

discussed, and recommendations concerning the applicability to particular scenarios are given.

2. Underwater Camera Modeling and Calibration

The theoretical basis for the 3D reconstruction of underwater objects using cameras in underwater housings is the multimedia photogrammetry (Maas 1995, Mulsow 2010). Kotowski presented a model that precisely describes the ray path when passing through different media (Kotowski 1988). This enables the use of collinearity equations for the reconstruction process of 3D points through appropriate extensions (Kotowski 1988, Maas 1995).

Many underwater calibration strategies are based on this model and attempt to reconstruct the exact ray path from the object point to the corresponding image point. However, due to the multiple refractions at the media transitions, the calculation formulas become complicated and the susceptibility to errors increases. This is due, among other things, to the fact that it cannot be guaranteed that all assumed boundary and secondary conditions apply. Examples of this include the assumptions of an orthogonal alignment of the camera to the viewing window, the homogeneity and uniform thickness of the glass material, or the accuracy of the refractive indices used. If these parameters deviate from the assumed values, this often cannot be detected, or the deviation cannot be precisely quantified.

Modeling the complete course of the rays considering refraction at the interfaces between water and glass, as well as between glass and air is described by Telem and Filin (2010), Sedlazeck and Koch (2011), Maas (1995), and Jordt et al. (2016).

Recent works using multimedia photogrammetry for the description of the geometry of underwater imaging systems and for realization of ray tracing in order to get valuable 3D reconstruction results are presented, e.g., by Kahmen and Rofallski (Kahmen et al. 2019, Kahmen et al. 2020, Rofallski et al. 2022, Rofallski and Luhmann 2022). Nocerino et al. introduce a solution for improvement of bundle adjustment in underwater

photogrammetry by distance dependent corrections (Nocerino et al. 2021). Elnashef and Filin introduce a refraction-invariant underwater calibration solution (Elnashef and Filin 2019).

The explicit modeling of the ray refraction at the boundaries of media leads to the general ray-based camera model, which may describe any arbitrary camera (Grossberg and Nayar 2005, Bothe et al. 2010). Hence, it is the most accurate basis to achieve a high accuracy 3D underwater measurement. Palomer introduces a calibration procedure for an underwater laser scanning system based on the ray-based camera model (Palomer et al. 2019).

The main reason for the rare use of the ray-based model is the challenging realization of a robust calibration procedure. Hence, many authors propose solutions which use the common pinhole model with extensions (e.g. Drap et al 2007). Lavest proposes an a-priori calibration without water contact (Lavest et al. 2003).

3. Underwater Calibration Approaches

To obtain a good 3D reconstruction of underwater objects using a stereo camera pair using the well-known triangulation principle, the underwater ray path of both cameras must be approximated as closely as possible. It is not important to describe the entire ray path from the object point to the corresponding pixel on the camera chip with geometric precision. Rather, it is sufficient to describe the part of the visual rays that runs in the water with geometric precision or to calculate a very good approximation.

For the goal of 3D object reconstruction with the highest accuracy, the purpose of underwater camera calibration is to achieve a description of the assignment of camera pixels to visual rays underwater that matches as close as possible to physical reality. This can be achieved, e.g., through a functional description with multiple parameters, which is a typical result of a camera calibration process. Otherwise, it can be obtained through a pixel-by-pixel ray description.

It is important to achieve both very good reconstruction accuracy and high robustness of the 3D calculation while maintaining a manageable calibration effort. Then, the underwater calibration process can be considered effective.

To achieve this goal, the calibration strategies described below were developed and investigated. The first calibration strategy (approach A1) is based on an approximation using a classic pinhole camera calibration and the construction of distance-dependent correction functions. The second strategy (approach A2) corresponds to the ray-based camera model in that a line of sight running through the water is determined and assigned to each camera pixel. The third strategy (approach A3) again uses a classic pinhole camera calibration. Additionally, the systematic measurement error is determined over the defined measurement volume (MV) and converted into a 3D correction function, which is applied to the measurement values.

3.1 Approach A1

The first approach is essentially based on calibration according to the pinhole camera model (PCM) and the determination of distance-dependent distortion functions. It is suitable when the properties and geometry of the stereo camera system are largely known due to design specifications or technical analysis, and an approximately orthogonal alignment of the cameras with respect to the respective viewing lenses can be achieved. If the system parameters are also known from an air calibration, the expected

underwater calibration can be estimated using an a priori analysis (Lavest et al. 2003, Bräuer-Burchardt et al. 2020). This a priori analysis should result in a reasonably good approximation of the underwater ray path using a conventional pinhole camera model calibration, at least for a certain distance range.

First, a conventional calibration of the stereo camera pair based on the pinhole camera model is performed in air without the underwater housing. Subsequently, the beam path is simulated underwater using the known design parameters (refractive index of the glass material, glass thickness, refractive index of the water in which the measurement is to be taken, distance of the camera from the viewing glass). Using these parameters, an extended pinhole camera calibration for the underwater case can be estimated (Bräuer-Burchardt et al. 2022a). This can be realized using a variable principal distance for every pixel radius to the principal point (see Bräuer-Burchardt et al. 2022b) or, alternatively, by different radially symmetric distortion functions for different object distances. An additional simulation can be used to estimate whether the changes across the measurement distance to be covered are significant or negligible for the 3D result. The resulting systematic measurement error, which can be extracted from the simulation calculation, can be reduced within certain limits by manipulating the camera distance from the viewing glass or, if possible, by changing the glass material or changing the glass thickness (Bräuer-Burchardt et al. 2022a).

Subsequently, a conventional calibration based on the pinhole camera model is performed underwater. Ideally, this calibration roughly corresponds to the a priori calculated calibration. In practice, there may be notable differences due to deviations from the assumed quantities or conditions. Therefore, underwater calibration is essential. Evaluation measurements, e.g., according to the VDI/VDE guideline (VDI/VDE, 2008), can be used to determine the remaining systematic error and thus quantitatively assess the quality of the calibration. If adjusting the design parameters is not feasible and the systematic residual error surpasses the desired tolerance level, the residual errors should be compensated by developing additional distance dependent distortion functions, e.g. as proposed by Nocerino et al. 2021. These functions can, for example, be determined experimentally by separate determination using special samples at defined measurement distances.

The calibration strategy proposed here corresponds in part to the methods proposed by (Lavest et al. 2003, Nocerino et al. 2021). Figure 1 shows a diagram of the complete proposed calibration process. Measurement examples for the achievable calibration quality are provided in Section 4.1.

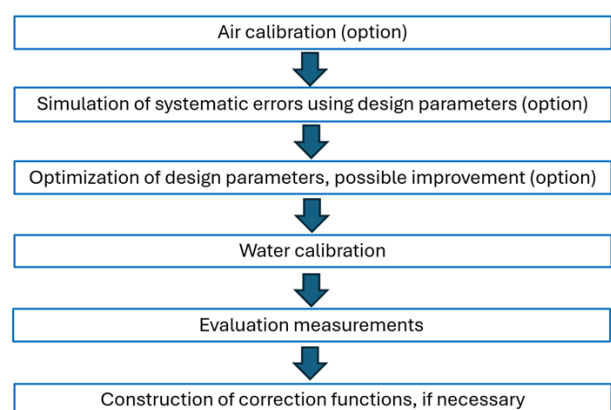


Figure 1. Scheme of the complete calibration process after A1.

3.2 Approach A2

This approach is based on the use of the ray-based camera model (RCM) for the two underwater cameras. Each pixel $p_{i,j}$ of a camera is assigned a line of sight $r^w_{i,j}$ in the water. Each line of sight is specified in a common world coordinate system (WCS). A line of sight can thus be described by a tuple $r^w_{i,j} = (x,y,z,u,v)_{i,j}$, where $(x,y,z)_{i,j}$ represents the starting point of a ray and $(u,v)_{i,j}$ represents the normalized 3D direction vector for pixel $p_{i,j}$. Each line of sight thus describes the ray path from an object point in the water to the first impact of the ray on another medium, i.e., in this case, the outside of the viewing glass of the underwater camera housing. The further ray path to the pixel on the camera chip does not need to be known for the 3D reconstruction of the object point.

The goal of the calibration process is to generate the line-of-sight descriptions for each camera pixel. For the 3D point calculation, corresponding image points from both camera images must then be found and the corresponding lines of sight intersected. This is done in the classical way (see Luhmann et al. 2006). For subpixel coordinates (x,y) of pixels p , the corresponding rays $r^w(p)$ are interpolated according to the following rule:

$$r^w(p) = w_{00}r^w_{x_0y_0} + w_{10}r^w_{x_1y_0} + w_{01}r^w_{x_0y_1} + w_{11}r^w_{x_1y_1} \quad (1)$$

where $r^w_{x_0y_0}, r^w_{x_1y_0}, r^w_{x_0y_1}, r^w_{x_1y_1}$ = rays corresponding to integer pixel co-ordinates next to p
 $w_{00}, w_{10}, w_{01}, w_{11}$ = corresponding weights with
 $w_{00} = (x_1-x) \cdot (y_1-y)$, $w_{10} = (x-x_0) \cdot (y_1-y)$,
 $w_{01} = (x_1-x) \cdot (y-y_0)$, and $w_{11} = (x-x_0) \cdot (y-y_0)$

We will give two proposals here for implementation of the calibration procedure. The first one uses three calibrations according to the pinhole camera model and the second one includes a high precision calibration plate which can be accurately placed in the calibration environment.

The following procedure is proposed for the calibration process, performing calibrations according to the pinhole camera model at three different distances. The aim is to generate the best possible approximation for a spatially very limited part of the measurement volume (a spatial plane) underwater using a pinhole camera model calibration. The theoretical basis for this is that an exact assignment of image point to object point for a spatial plane using the pinhole camera model, including distortion functions, is possible even underwater (see Bräuer-Burchardt et al. 2022a). Starting with an initial reference calibration (RC), which determines the parameters for a spatial plane in the central part of the measurement volume, two further calibrations are performed at the front (NC) and rear (FC) border.

The external orientation between the two stereo cameras is adopted from the first calibration and fixed, i.e., assumed to be correct. This means that for the NC and FC calibrations, the deviations from RC must be described exclusively using the internal parameters and the distortion functions. The ray-based representation is then obtained by placing two virtual planes (PN and PF) at constant Z-Values in the WCS, one at the front boundary (PN at Z_N) of the measurement volume and one at the rear boundary (PF at Z_F). The orientation of the cameras is approximately in direction of the Z-axis of the WCS. The parameters $(x,y,z)_{i,j}$ correspond to the intersection points of the calibration NC with PN, and the $(u,v)_{i,j}$ result from the differences between the intersection points of FC with PF and NC with PN, each for both cameras (see fig. 2):

$$u_{i,j} = \frac{(x_{i,j,F} - x_{i,j,N})^2}{L^2}; v_{i,j} = \frac{(y_{i,j,F} - y_{i,j,N})^2}{L^2} \quad (2)$$

with $L = \sqrt{D^2 + (x_{i,j,F} - x_{i,j,N})^2 + (y_{i,j,F} - y_{i,j,N})^2}$
 where $D = Z_F - Z_N$ = distance between planes PF and PN
 $(x,y)_{i,j,N}$ = 3D intersection point of the ray $r(p,N)$ corresponding to NC and integer pixel $p_{i,j}$ with PN
 $(x,y)_{i,j,F}$ = 3D intersection points of the ray $r(p,F)$ corresponding to FC and integer pixel $p_{i,j}$ with PF.

A second variant for generating the beam tuples $r^w_{i,j} = (x,y,z,u,v)_{i,j}$ without performing conventional PCM calibrations consists of recording a flat calibration plate at distances DN and DF in water. The calibration plate should be approximately flat (made of a solid material, e.g., glass or granite). Furthermore, it must contain a defined pattern of lines, points, circles, or markers that enables highly accurate position estimation for all image points on the calibration plate. This plate must also be precisely positioned in order to be able to describe the second position with high accuracy in the WCS with respect to the first position. The calibration procedure would then be as follows: an image of the calibration plate is recorded at each position DN and DF with both cameras, and the original positions of the image points on the calibration plate are determined. This simultaneously determines the positions in the WCS, from which the beam tuples can be calculated, analogous to the first variant.

To reduce measurement uncertainty, it is recommended to capture entire image sequences without moving the cameras or the calibration plate and to average the calculated object positions. Due to its ease of use, this method is recommended for applications in water tanks where the mechanical capabilities for precise panel positioning exist. The advantage of this technique is that it eliminates the risk of incorrect approximate calibrations using the pinhole camera model. The disadvantage is the very high mechanical requirements placed on the calibration plates (strength, pattern accuracy) and their positioning. Furthermore, it must be accepted that only a limited number of pixels can be measured accurately, and the remainder must be interpolated.

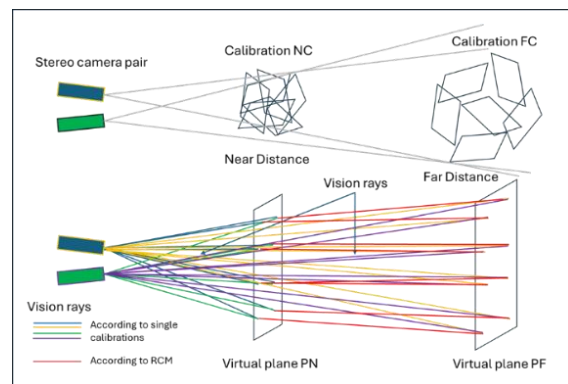


Figure 2. Sketch of the calibration situation of A2.

3.3 Approach A3

The third approach again uses a classical PCM calibration in water. Furthermore, measurements of ball-bars and plane-specimens are conducted to assess the systematic error of the measurements across various regions in the MV. These errors should be described by certain functions over the measurement volume, e.g., by polynomials. Determination of the error function is achieved as follows. Initially, the MV is defined, and a 3D grid of equidistant sampling points is defined.

Measurements of ball-bars are performed at as many positions in the measurement volume as possible. According to the known length of the ball-bar, the length error ΔL is determined for each position. Subsequently ΔL is split into two vectors of equal length with opposite orientation (see fig. 3): $\Delta L = |v_1| + |v_2|$. Alternatively, positioning of the ball-bars can be performed in such a way that one of the spheres is always in the approximate center C_{MV} of the measurement volume. It is assumed that the systematic error is negligible at C_{MV} . The determined length measurement error is transformed into an error vector at the position of the second sphere. Using this arrangement, it is meaningful to use ball-bars of different lengths.

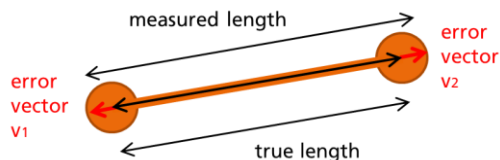


Figure 3. Splitting of the length error for sampling it in the measurement volume for averaging.

The error vectors are stored and used for estimation and averaging of the error at neighboring sampling points. The values of the averaged error vectors are the input for the estimation of an error polynomial or an interpolation error function.

4. Experimental Evaluation

4.1 Experiments according to approach A1

The calibration according to approach A1 has been applied to several underwater scanner systems in the past. The first system is a handheld scanner for close-range 3D acquisition (Bräuer-Burchardt et al. 2016). The measurement volume is approximately $300 \times 200 \times 100 \text{ mm}^3$. The other two scanners investigated are ROV-based systems with measurement volumes of just under 1 m^3 . The measurement accuracy was determined according to the VDI/VDE guidelines (VDI/VDE, 2008).

All systems achieved very good results in terms of achievable measurement accuracy when calibrated with the extended pinhole camera model. The maximum systematic measurement error across the respective measurement volume was less than $1/2000$ of the measurement volume diagonal. The detailed measurement results are documented in (Bräuer-Burchardt et al. 2016), (Bräuer-Burchardt et al. 2020), (Bräuer-Burchardt et al. 2022a), and (Bräuer-Burchardt et al. 2024).

The results show that the calibration procedure is suitable if the necessary technical conditions are met, i.e., there is no excessive variation in distortion across the possible measurement distances. This can be estimated a priori through simulations with knowledge of the sensor geometry.

4.2 Experiments according to approach A2

Calibration of a stereo camera setup according to the ray-based camera model has been successfully tested using a laboratory setup in air (Bräuer-Burchardt et al., 2022b). Using wide angle lenses, the systematic error could be reduced by a factor of about four. Initial experiments to perform ray-based camera calibration under water have been performed in a laboratory setup using an aquarium. The size of the aquarium was $1500 \times 500 \times 600 \text{ mm}^3$ (length x width x height). The camera pair was placed outside the

aquarium with a short distance to the glass. The measurement volume was defined as the hole inner part of the aquarium with a minimum distance of 700 mm to the cameras. A photograph of the setup is shown by fig. 4.



Figure 4. Aquarium test setup with the ArUco marker board placed in the water for calibration.

Three calibrations have been performed using a calibration board with ArUco markers and circles (see fig. 5 left) at mean distances of 700 mm (front), 1050 mm (medium), and 1400 mm (rear), respectively. Hence, three sets of calibration parameters NC, RC, and FC were obtained.

Measurements of a ball-bar (Fig. 5 right) with a calibrated sphere center distance of 250.242 mm and sphere radii of about 37.5 mm each were carried out using structured illumination with aperiodic fringe patterns generated by a digital projector.

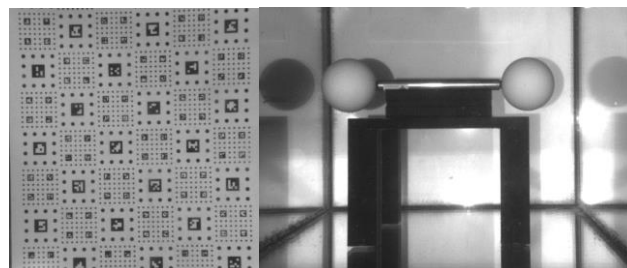


Figure 5. ArUco marker board (left) and ball-bar (right).

The ball-bar was placed in the aquarium at distances between 650 mm to 1350 mm in 100 mm intervals. Sequences of fringe images were recorded. These image sequences served as input for a 3D reconstruction of the scene. The 3D measurements were performed using the different calibration parameter sets NC, RC, and FC, generating a total of $3 \times 8 = 24$ measurement data sets. The sphere center distance and sphere radii were determined using the in-house software "Argus."

The results for the sphere center distances are documented in Table 1. It is noticeable that large systematic measurement errors only occur at close range when the 3D data were calculated using the FC calibration. Unexpectedly, all three calibrations yield acceptable results at greater measurement distances. However, the noise in the 3D points escalates disproportionately with increasing distance, indicating other previously overlooked error sources, such as reflections from the aquarium's glass wall. Additionally, errors in point assignment may arise. A careful error analysis should be conducted in future studies.

Calibration Distance [mm]	NC	RC	FC
650	250.47	251.16	249.14
750	250.03	250.71	247.81
850	249.95	250.27	247.88
950	250.11	250.23	248.73
1050	250.05	250.03	249.19
1150	249.86	249.81	249.64
1250	250.09	249.82	250.25
1350	250.13	249.70	250.66

Table 1. Results of ball-bar length measurements in mm

The fixing of the extrinsic parameters of both cameras according to the medium calibration did not successfully result in valid calibrations for the other distances. Hence, a combination of near and far calibration did not directly lead to the ray-based representation according to the ray-tuples. To realize a combination of NC and FC for calculation of the 3D object points, weighted length measurement values (WLV) were combined. The weights were determined using the mean calculated distances of the object points. The results are documented in table 2. Figure 6 illustrates the length measurement error depending on the measurement distance using NC, RC, FC, and the weighted measurements.

Distance [mm]	WLV [mm]	ΔL_w
650	250.47	0.23
750	249.87	-0.37
850	249.51	-0.73
950	249.62	-0.62
1050	249.62	-0.62
1150	249.72	-0.52
1250	250.22	-0.02
1350	250.62	0.38

Table 2. Values of weighted length measurements

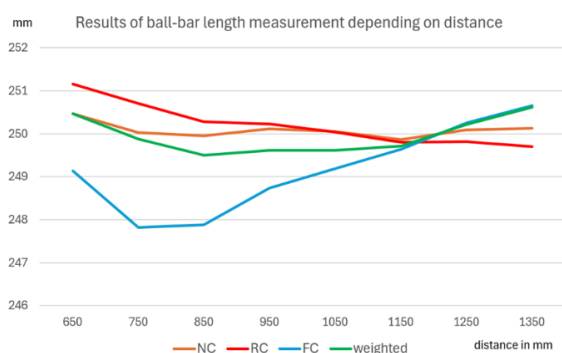


Figure 6. Estimated systematic errors of length measurements depending on measurement distance and calibration.

4.3 Experiments according to approach A3

Approach A3 has been previously tested using a laboratory setup in air (Bräuer-Burchardt et al., 2018). It was shown that the systematic error could be reduced by a factor of about two. Application under water performs analogously to the case in air as well. The same laboratory setup as for the experiments concerning approach A2 was used for a first approximation of the systematic error function over the measurement volume. Unfortunately, the number of valid ball-bar measurements was

too small for a certain estimation of the error function over the whole measurement volume. However, a simple spreading function which should be applied to the calculated object point co-ordinates was determined using the ball-bar measurements. This correction function reduced the systematic measurement error of the ball-bar measurements compared to the uncorrected variant.

5. Summary, Discussion, and Outlook

Three approaches for calibration strategies for an optical underwater 3D stereo scanner with low effort, easy handling and expected high accuracy were proposed. All proposed calibration strategies provide a simple applicability and may provide satisfactory measurement results.

The use of an extended pinhole camera model for underwater calibration according to approach A1 offers high accuracy potential but requires a careful a priori analysis of the geometric conditions. Suitability should be clarified in advance through appropriate simulations or theoretical calculations of the ray paths. A practical evaluation through a real underwater calibration process is necessary, since the validity of all assumed conditions cannot be guaranteed.

The main advantage of A1 is the ability to perform a trusted procedure as known from classical air calibrations. However, the selected components and the geometric construction and arrangement of the cameras inside the underwater scanner system must fit. This can typically be achieved by a certain mechanical construction of the system including camera and underwater housing.

The ray-based approach A2 offers the highest accuracy potential, as theoretically the actual ray geometry is used for the 3D calculations. However, a robust and precise calibration is difficult to implement. The proposed approach, a combination of two pinhole camera model calibrations for limited distance ranges, is inexpensive to implement, but unfortunately susceptible to various error influences. Therefore, further research is needed in this area. Firstly, a simulation model should be generated and tested to exclude error influences in the modeling and calculation. Additionally, further extensive experimental investigations in operational environments (e.g., in large water basins) are required.

Approach A2 promises general applicability for underwater stereo systems, also when using spherical dome ports. The effort compared to the case in air is manageable.

Approach A3 is somewhat of an improvised solution. However, the effort is restricted and clear, and a certain reduction of the systematic error is expected.

Future work should be addressed mainly to the experimental evaluation of strategies A2 and A3 and assessment of the effort in relation to the achievable measurement accuracy. Additionally, different strategies should be compared using the same laboratory equipment under equal conditions during the underwater calibration process. This comparison should consider the technical and personnel effort, as well as the time required for the entire calibration process. Furthermore, an evaluation should be conducted according to VDI/VDE standards, and various test objects with relevant dimensions or shapes should be measured three-dimensionally. The different calibrations are then applied to the same measurement data, allowing a direct comparison of the measurement data.

References

- Bothe, T., Li, W., Schulte, M., von Kopylow, C., Bergmann, R.B., Jüptner, W., 2010. Vision ray calibration for the quantitative geometric description of general imaging and projection optics in metrology. *Appl Opt* Vol. 49(30), 5851-5860.
- Bräuer-Burchardt, C., Heinze, M., Schmidt, I., Kühmstedt, P., Notni, G., 2016. Underwater 3D surface measurement using fringe projection based scanning devices. *Sensors* 2016, 16(1), 13; doi:10.3390/s16010013.
- Bräuer-Burchardt, C., Kühmstedt, P., Notni, G., 2018. Improvement of measurement accuracy of optical 3D scanners by discrete systematic error estimation, in: R. P. Barneva et al. (Eds.): *Proc IWCIA 2018, LNCS 11255*, pp. 202–215.
- Bräuer-Burchardt, C., Munkelt, C., Gebhart, I., Heinze, M., Heist, S., Kühmstedt, P., Notni, G., 2020. A-priori calibration of a structured light projection based underwater 3D scanner. *Journal of Marine Science and Engineering* 8(9): 635, DOI:10.3390/jmse8090635.
- Bräuer-Burchardt, C., Munkelt, C., Heinze, M., Gebhart, I., Kühmstedt, P., Notni, G., 2022a. Underwater 3D Measurements with Advanced Camera Modelling. *PFG* 90, 55–67. <https://doi.org/10.1007/s41064-022-00195-y>.
- Bräuer-Burchardt, C.; Ramm, R.; Kühmstedt, P.; Notni, G., 2022b. The duality of ray-based and pinhole-camera modeling and 3D measurement improvements using the ray-based model. *Sensors* 2022, 22, 7540. <https://doi.org/10.3390/s22197540>.
- Bräuer-Burchardt, C.; Munkelt, C.; Bleier, M.; Baumann, A.; Heinze, M.; Gebhart, I.; Kühmstedt, P.; Notni, G., 2024. Deepwater 3D measurements with a novel sensor system. *Appl. Sci.* 2024, 14(2), 557; <https://doi.org/10.3390/app14020557>.
- Drap, P., Seinturier, J., Scaradozzi, D., Gambigi, P., Long, L., Gauch, F., 2007. Photogrammetry for virtual exploration of underwater archaeological sites. In: *Proceedings of the XXI CIPA Symposium*.
- Elnashef, B. and Filin, S., 2019. Direct linear and refraction-invariant pose estimation and calibration model for underwater imaging. *ISPRS Journal of Photogrammetry and Remote Sensing*, Vol 154(8) 2019, 259-271.
- Grossberg, M.D., Nayar, S.K., 2005. The raxel imaging model and ray-based calibration, *IJCV* 61(2), 119-137.
- Jordt, A., Köser, K., Koch, R., 2016. Refractive 3D reconstruction on underwater images. *Methods in Oceanography*, 15-16. pp. 90-113. DOI 10.1016/j.mio.2016.03.001.
- Kahmen, O., Rofallski, R., Conen, N., Luhmann, T., 2019. On scale definition within calibration of multi-camera systems in multimedia photogrammetry. In: *Int. Arch. Photogramm. Remote Sens. Spatial Inf. Sci.* XLII-2/W10, 93–100. DOI: 10.5194/isprs-archives-XLII-2-W10-93-2019.
- Kahmen, O., Rofallski, R., Luhmann, T., 2020. Impact of stereo camera calibration to object accuracy in multimedia photogrammetry. In: *Remote Sensing* 12 (12), S. 2057–2087. DOI: 10.3390/rs12122057.
- Kotowski, R., 1988. Phototriangulation in multi-media photogrammetry. *Int. Arch. Photogramm. Rem. Sens.* 27, 324-334.
- Lavest J.M., Rives, G., Lapreste, J.T., 2003. Dry camera calibration for underwater applications. *Machine Vision and Applications* 2003, 13: 245–253.
- Luhmann, T., Robson, S., Kyle, S., Harley, I., 2006. *Close range photogrammetry*. Wiley Whittles Publishing.
- Maas, H.G., 1995. New developments in multimedia photogrammetry. In: *Optical 3-D Measurement Techniques III*. (Eds.: A. Grün, H. Kahmen), Wichmann Verlag, Karlsruhe.
- Maas, H.G., 2015. On the accuracy potential in underwater/multimedia photogrammetry. *Sensors* 2015, 15(8), 1814-1852.
- Menna, F., Agrafiotis, P., Georopoulos, A., 2018. State of the art and applications in archaeological underwater 3D recording and mapping. *J. Cult. Herit.* 33, 231–248.
- Mulsow, C., 2010. A flexible multi-media bundle approach. *Int Arch Photogramm. Rem. Sens. Spat. Inf. Sci.*, XXXVIII/5, 472-477.
- Nocerino, E., Menna, F., Gruen, A., 2021. Bundle adjustment with polynomial point-to-camera distance dependent corrections for underwater photogrammetry, *Int. Arch. Photogramm. Remote Sens. Spatial Inf. Sci.*, XLIII-B2-2021, 673–679, <https://doi.org/10.5194/isprs-archives-XLIII-B2-2021-673-2021>.
- Palomer, A., Ridao, P., Forest, J., Ribas, D., 2019. Underwater laser scanner: ray-based model and calibration. *IEEE/ASME Trans Mechatronics*, Vol. 24, No. 5, 1986-1997
- Rofallski, R., Luhmann, T., 2022. An efficient solution to ray tracing problems in multimedia photogrammetry for flat refractive interfaces. *PFG – J. Photogramm. Rem. Sens. Geoinf. Sci.*
- Rofallski, R., Kahmen, O., Luhmann, T., 2022. Investigating distance-dependent distortion in multimedia photogrammetry for flat refractive interfaces. In: *Int. Arch. Photogramm. Remote Sens. Spatial Inf. Sci.* XLVIII-2/W2-2022, S. 127–134. DOI: 10.5194/isprs-archives-XLVIII-2-W2-2022-127-2022.
- Sedlazeck, A., Koch, R., 2011. Perspective and non-perspective camera models in underwater imaging - overview and error analysis. In: *Theoretical Foundations of Computer Vision*, vol. 7474 of Springer LNCS, 212–242.
- Shortis, M., 2015. Calibration techniques for accurate measurement by underwater camera systems. *Sensors* 2015, 15(12), 30810-30826.
- Shortis, M., 2019. Camera calibration techniques for accurate measurement underwater. In *3D Recording and Interpretation for Maritime Archaeology*; Coastal Research Library; McCarthy, J., Benjamin, J., Winton, T., van Duivenvoorde, W., Eds.; Springer: Cham, Switzerland; Volume 31.
- Telem, G., Filin, S., 2010. Photogrammetric modeling of underwater environments, *ISPRS Journal of Photogrammetry and Remote Sensing* 65(5), 433-444.
- VDI/VDE, 2008. *VDI/VDE 2634. Optical 3D-measuring systems. VDI/VDE guidelines, Part 2*.